Marine Geology 475 (2024) 107365

Contents lists available at ScienceDirect

Marine Geology

journal homepage: www.elsevier.com/locate/margo

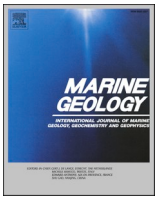

Research Article

Tropical cyclone activity over the past 1200 years at the Pelican Cays, Belize

Chris L. Blanco [a,*], Andrea D. Hawkes [a], Elizabeth J. Wallace [b], Jeffrey P. Donnelly [c], Dana MacDonald [d]

[a] Department of Earth and Ocean Sciences, Center for Marine Science, University of North Carolina Wilmington, Wilmington, NC, USA
[b] Department of Earth and Ocean Sciences, Old Dominion University, Norfolk, VA, USA
[c] Department of Geology and Geophysics, Woods Hole Oceanographic Institution, Woods Hole, MA, USA
[d] Department of Earth, Geographic, and Climate Sciences, University of Massachusetts, Amherst, MA, USA

ARTICLE INFO

Editor: Shu Gao

Keywords:
Paleotempestology
Tropical cyclones
Belize
Climate
Random variability
Western Caribbean

ABSTRACT

Tropical cyclone (TC) models indicate that continued planet warming will likely increase the global proportion of powerful TCs (specifically Categories 4 and 5 hurricanes), increasingly jeopardizing low-lying coastal communities and resources such as the Pelican Cays, Belize. The combination of increased coastal development and continued relative sea-level rise puts these communities at even higher risk of damage from TCs. The short TC observational record for the western Caribbean hampers the extensive study of TC activity on centennial timescales, which hinders our ability to fully understand past TC climatology and improve the accuracy of TC models. To better assess TC risk, paleotempestological studies are necessary to put future scenarios in perspective. Here, we present a high-resolution reconstruction of coarser-grained sediment deposits associated with TC (predominately ≥ Category 2 hurricanes) passages over the past 1200 years from Elbow and Lagoon Cays, two coral reef-bounded lagoons at the northern and southern end of the Pelican Cays; the most southern Belizean paleotempestological site to date. Coincident timing of historic storms with statistically significant coarser-grained deposits within cay lagoon sediment cores allows us to determine which historic TCs likely generated event layers (tempestites) archived in the sediment record. Our compilation frequency analysis indicates one active interval (above-normal TC activity) from 1740-1950 CE and one quiet interval (below-normal TC activity) from 850-1018 CE. The active and quiet intervals in the Pelican Cays composite record are anticorrelated with those from nearby and re-analyzed TC records to the north, including the Great Blue Hole (~100 km north) and the Northeast Yucatan (~380 km northwest). This site-specific anticorrelation in TC activity along the western Caribbean indicates that we cannot rely on any one single TC record to represent regional TC activity. However, we cannot discount that these anticorrelated periods between the western Caribbean sites are due to randomness. To confirm that the anticorrelation in TC activity among sites from the western Caribbean is indeed a function of climate change and not randomness, an integration of more records and TC model simulations over the past millennium is necessary to assess the significance of centennial-scale variability in TC activity recorded in reconstructions from the western Caribbean.

1. Introduction

1.1. Socioeconomic effects and future projections of tropical cyclones

Understanding how tropical cyclone (TC) patterns might change under future warming scenarios is vital due to the devastating societal effects that TCs can inflict (Knutson et al., 2020). Flooding and storm surge from TCs disproportionately affect vulnerable human and ecological systems that are least equipped to recover (Brouwer et al., 2007). TCs are the costliest natural disaster, amounting to $2 trillion in normalized 2018 CE United States (US) economic losses from 1900 to -2017 CE, equating to just under $17 billion annually on average (Weinkle et al., 2018). The 2017 CE Atlantic TC season alone caused more than $250 billion in damages and killed thousands throughout the Caribbean, US Southeast, and Southern Great Plains (Kishore et al., 2018). In 2018 CE, TCs Florence and Michael caused $50 billion in

* Corresponding author at: University of North Carolina Wilmington, Center for Marine Science, 5600 Marvin K. Moss Lane, Wilmington, NC 28409, USA.
E-mail address: clb1111@uncw.edu (C.L. Blanco).

https://doi.org/10.1016/j.margeo.2024.107365
Received 2 October 2023; Received in revised form 14 July 2024; Accepted 22 July 2024
Available online 25 July 2024
0025-3227/

damage and killed hundreds of people (Beven et al., 2019; Stewart and Berg, 2018). Recent Atlantic TC seasons have been particularly active with 2019 CE marking the fourth consecutive above-normal Atlantic TC season, and 2020 CE had a record number of storms (30 named storms). The most recent projections of TC activity indicate that in a + 2 °C-warmer world, damage from TCs will increase with higher storm surge associated with increased rates of relative sea-level rise and precipitation (Knutson et al., 2020). Concurrently, Knutson et al. (2020) project a 13% increase in the frequency of Category 4 and 5 TCs, 5% increase in TC wind speeds, and a gradual poleward migration of TC tracks.

Belize has many coastal and cay communities that are at risk of devastating TC strikes. These coastal communities are spread along the entire Belize coastline (~390 km). In the last two decades, there have been anthropogenic modifications and construction on offshore cays such as the Pelican Cays (Macintyre et al., 2009; Fig. 1d inset), coinciding with a lull in landfalling Belize TCs (the last landfalling major TC was Category 4 Iris in 2001 CE and the last major TC to pass within 100 km of Belize was Category 5 Dean in 2007 CE). Additionally, the overall wealth of Belize is linked to the health of the tourism industry (Key, 2002). Thus, TC strikes jeopardize both the wellbeing of Belize's coastal population and economy. In fact, Belize's most densely populated coastal city, Belize City, was devasted by Category 4 TC Hattie in 1961 CE. Hattie was responsible for 319 fatalities and $60.3 million in damages (1961 USD; Nancoo, 1962). Since 1851 CE, six major TCs (Iris, 2001 CE; Keith, 2000 CE; Greta, 1978 CE; Hattie 1961 CE; Janet, 1955 CE, Unnamed 1931 CE) made landfall in Belize resulting in a recurrence interval of one every 28.5 years. These storms resulted in major economic damage and human casualties. For example, Category 4 TC Iris in 2001 CE produced $250 million (in 2001 USD) in damages, 36 direct fatalities, and left 15,000 people homeless (Avila, 2001). To further contextualize these powerful and devastating storms, it is vital to extend the Belize TC record using high resolution proxy reconstructions.

1.2. Paleotempestology of Belize and other nearby sites

TC risk assessments in the Atlantic mostly rely on NOAA's reanalyzed 'best track' instrumental TC dataset which includes all TCs occurring from 1851 CE-present (Landsea et al., 2008; Knapp et al., 2010; Knutson et al., 2010; Knutson et al., 2020). This 173-year archive captures regional anticorrelation in TC patterns and frequency, particularly in the variability of ≥Category 2 TCs, across islands (< 300 km apart) in the Bahamas (Winkler et al., 2020, 2022). However, the instrumental record is still too short and incomplete in many regions of the world, especially the western Caribbean (which includes Central American countries such as Mexico, Belize, Honduras, and Guatemala) to explain the potential effect that climate forcings have on changing TC patterns on longer timescales (Knutson et al., 2010, 2020). Thus, paleotempestological records are necessary in the examination of how certain climate forcings might influence TC activity.

To date, there are seven published paleotempestological sediment records from Belize (Gischler et al., 2008, 2013; McCloskey and Keller, 2009; McCloskey, and Liu, K.-biu., 2012; Denommee et al., 2014; Adomat and Gischler, 2016; Schmitt et al., 2020), and one published paleotempestological record from the Northeast Yucatan, Mexico (Sullivan et al., 2022). Three of the seven Belize studies analyzed sediment cores collected from wetlands and marshes along the central coast to reconstruct lower-resolution (centennial to millennial) ~5000–8000-yr records of Belize TC activity (McCloskey and Keller, 2009; McCloskey, and Liu, K.-biu., 2012; Adomat and Gischler, 2016). The other four studies analyzed sediment cores collected from the Great Blue Hole at Lighthouse Reef, Belize to reconstruct a Common Era (0 CE-present) record of Belize TC activity (Gischler et al., 2008, 2013; Denommee et al., 2014; Schmitt et al., 2020). The Northeast Yucatan study analyzed two sediment cores collected from Cenote Muyil (a coastal sinkhole), Lake Chunyaxche, Mexico.

Additionally, a common geochemical approach in paleotempestology includes the use of speleothems, such as stalagmites and stalactites found in caves. Speleothems can be used to infer changes in precipitation patterns and hydroclimate variability, which can indirectly reflect variations in TC activity (Pollock et al., 2016; Obrist-Farner et al., 2023). This inferred TC-signal is very complicated and is likely muddled by non-TC precipitation regimes in the region which are influenced by changes in the Intertropical Convergence Zone (ITCZ), the eastern tropical Pacific and Caribbean sea surface temperatures (SSTs), the strength of the Caribbean Low Level Jet (CLLJ), the westward expansion of the North Atlantic Subtropical High (NASH; Anderson et al., 2019; Martinez et al., 2019; Obrist-Farner et al., 2023) and steep topographic gradients between sampling sites (Imbach et al., 2018). Frappier et al. (2007b) analyzed stalagmite $\delta^{18}O$ and $\delta^{13}C$ values at high-resolution (weekly-monthly) and linked excursions in these isotope records to specific historical TCs ranging in intensity from tropical storm to major hurricane, and with storm tracks whose eyes passed the cave within 40–370 km (Frappier et al., 2007). This geochemical approach is useful, however, the main drawback is the temporal limitation of the record, for example, the high-resolution stalagmite isotope record from Frappier et al. (2007b) only reflects ~30 years of precipitation patterns.

When comparing TC frequency along western Caribbean sites, we focus on the latter two (and most recent) Belize records, which reconstructed (near-) annually resolved Common Era TC activity (Denommee et al., 2014; Schmitt et al., 2020), and the high-resolution record from the Northeast Yucatan, Mexico (Sullivan et al., 2022). Denommee et al. (2014) identified two active intervals (800–1350 CE and 1900 CE-present) and one quiet interval (1400–1880 CE), whereas Schmitt et al. (2020) identified an overall shift in TC frequency from a quiet and stable interval from 100-900 CE to a more active and variable interval from 1100 CE-present. Sullivan et al. (2022) identified four active intervals (215 BCE-80 CE, 755–825 CE, 975–985 CE, and 1285–1420 CE) and three quiet intervals (315–435 CE, 590–650 CE, and 1495–1745 CE) in their combined Cenote Muyil record. Despite using the same blue hole to reconstruct Common Era Belize TC activity, the Great Blue Hole records from Denommee et al. (2014) and Schmitt et al. (2020) do not correlate in the magnitude of TC events. Inconsistencies in reconstructed TC activity for the Great Blue Hole could be explained by differences in sediment core age control, and methodological criteria for identifying TC event layers and calculating event frequencies (see Schmitt et al., 2020 for a full description of methods). The age model for the Denommee et al. (2014) record shows a consistent ~339-yr offset between varve counts and ^{14}C ages in the sediment record. The record from Schmitt et al. (2020) is missing the first ~88 years due to liquification of the top 74 cm of sediment during sampling (Schmitt personal communication). The record from Schmitt et al. (2020) is annually resolved based on varve counting (corroborated by ^{14}C dating) and they used a five-point multi-proxy approach for identifying event layers: (1) grain size > 20–24 μm; (2) < 85% of fine material < 63 μm; (3) layer thickness > 2.5 mm; (4) yellow/brown colour; and (5) Sr/Ca-ratio > 0.025 (Schmitt et al., 2020). Denommee et al. (2014) identified event layers based on visual observation (i.e., grain size, layer thickness, and colour).

We present a new high-resolution reconstruction of TC activity over the past 1200 years from the Pelican Cays, Belize, a re-analyzed composite record from the Northeast Yucatan (Sullivan et al., 2022), and re-analyzed Great Blue Hole records (Denommee et al., 2014; Schmitt et al., 2020) to alleviate the current inconsistencies in the records from the Great Blue Hole, and to evaluate the regional signal of TC activity between sites in the western Caribbean. This is possible because our cores from Pelican Cays (Elbow and Lagoon Cay) have high mean sedimentation rates (0.5 cm/yr) and unique geographic position, sitting ~100 km southwest of the Great Blue Hole and ~390 km south of the Northeast Yucatan (Fig. 1a).

2. Study area and methods

Belize is a tropical country located on the northeastern coast of

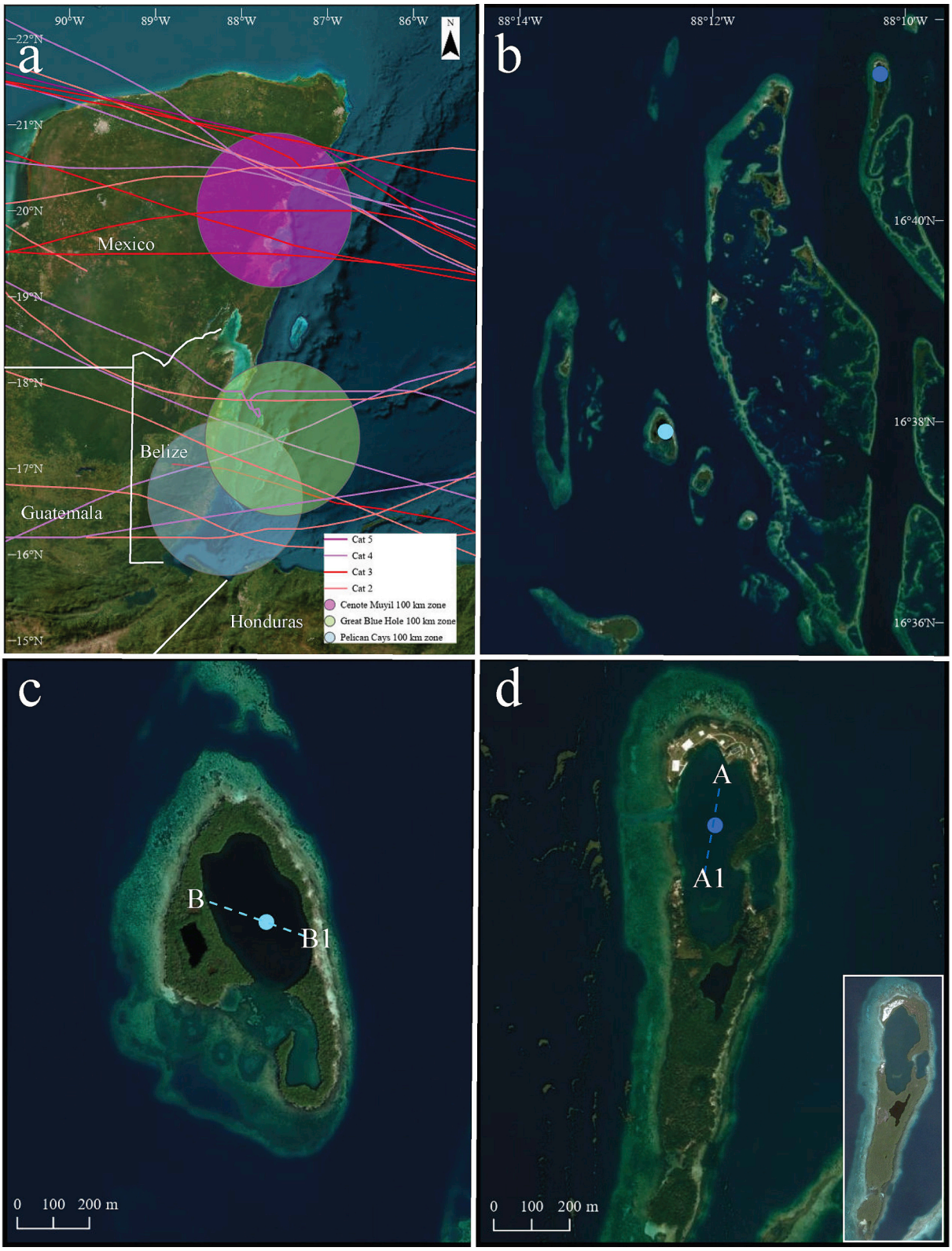

Fig. 1. (a) Regional study site showing historic (1851–2007 CE) tropical cyclones (≥ Category 2) track lines passing within a 100 km-radius of the Pelican Cays (blue circle), Great Blue Hole (green circle), and Cenote Muyil (purple circle). Track line colour corresponds to the strength of the storm when it passed within 100 km of each site. (b) Location of Elbow (toward the northern end) and Lagoon Cay (toward the southern end) within the Pelican Cays. (c, d) Lagoon Cay core site (16.631468° N; 88.207906° W) and Elbow Cay core site (16.691043° N; 88.171182° W) indicated by teal and blue colored dots, respectively. Dashed lines are StrataBox seismic profile track lines (see Fig. S1 for full seismic profile). (d; inset) 2006 CE satellite imagery of Elbow Cay showing little development compared to 2021 CE imagery (Google Earth). (For interpretation of the references to colour in this figure legend, the reader is referred to the web version of this article.)

Central America (Fig. 1a). The Pelican Cays are collectively made up of a dozen reef-bounded cays on the western side of the Belize Barrier Reef (Fig. 1b). Elbow Cay and Lagoon Cay occupy the northern and southern end of the Pelican Cays, respectively (Fig. 1b) and mangroves fringe both cays, which bound 14.7 m (Elbow) and 15 m (Lagoon) deep central lagoons (Fig. 1c, d; Fig. S1). Elbow Cay also has a smaller eastern lagoon (200 m long and 100 m wide; Fig. 1d). Access to Elbow Cay is via a shallow (<1 m deep) and narrow (30 m wide) channel opening to coastal waters on its western edge that was anthropogenically excavated between 2006 and 2010 CE (Google Earth; Fig. 1d). Lagoon Cay has a shallow (1 m) 85-m wide opening to coastal waters on its southern edge (Fig. 1c). Stratigraphy from vibracores collected in 2009 CE at Elbow Cay (ELB; 502 cm) and Lagoon Cay (LGN; 529 cm; Fig. 1b-d; Fig. S1) are dominated by light grey (2.5Y 7/1) sediments ranging from clay to very coarse sand.

During the historic period (1851–2007 CE), the Pelican Cays experienced 17 tropical storms, seven Category 1, three Category 2, one Category 3, and three Category 4 tropical cyclones (TCs) within a 100-km radius (TCs_{100km}). We focus on the 14 TCs_{100km} (≥ Category 1) when correlating historic TCs to event layers in the ELB and LGN sediment cores from the Pelican Cays. By tying event layers to specific TCs in the historic period, we can begin to understand the types of storms (and storm characteristics) that are conducive to generating large waves breaching the mangrove barriers of Elbow Cay and Lagoon Cay and producing event layers over the last 1200 years. However, lesser-magnitude storms, such as tropical storms, can also generate event layers in this mangrove-cay environment, especially when passing south of the Pelican Cays, where the greatest fetch for a TC's stronger northeasterly winds occurs.

2.1. Sediment core chronology

We applied ^{137}Cs and ^{14}C dating to ELB and LGN sediment cores to establish independent chronologies. We analyzed sediment samples at five-cm intervals from 0-40 cm using gamma detection to broadly identify ^{137}Cs activity. We then analyzed sediment samples at one-cm intervals from 10.5-23.5 cm in ELB and from 23.5-27.5 cm in LGN to pinpoint the precise depth at which ^{137}Cs peaked, indicating ~1963 CE (Figs. S3 and S4). We derived chronological control deeper in the cores by applying ^{14}C dating to terrestrial plant macrofossils (red mangrove leaves and plant matter), marine carbonates, and in situ coral at the National Ocean Science Accelerator Mass Spectrometer facility. We performed traditional, higher-resolution AMS dating on plant macrofossils (one sample each for ELB and LGN) and coral (one sample for ELB), while gas bench dating was used for bulk carbonate for the remaining age horizons (six dates in ELB and five in LGN; Table S1). We produced age-depth models in Bacon (version 4.1.0) using all ^{14}C dates and ^{137}Cs calendar dates from ELB and LGN sediment cores (Table S1; Blaauw and Christen, 2011, 2013). Bacon calibrated the ^{14}C dates using CALIB's IntCal20 calibration curve for the mangrove samples (Reimer et al., 2020) and CALIB's Marine20 calibration curve for the carbonate and coral samples (Heaton et al., 2020). We used a local marine reservoir correction of 157 ± 26 years from the nearest available site, Glover's Reef, Belize (~43 km to the north of the Pelican Cays; Druffel, 1980), on the carbonate and coral samples.

2.2. Sediment and statistical analyses

2.2.1. Grain size analysis

We ran grain size analysis on cores ELB and LGN at 1 cm-intervals using a Beckman Coulter laser particle size analyzer. There was no visual or stratigraphic indication of event layers (i.e., visible coarser layers intercalated into the finer-grained background sediment) in ELB or LGN (Figs. S1; S2). We identified event layers based on the percent sand data (>63 μm) of each sediment sample following the procedures of Donnelly et al. (2015) and Wallace et al. (2019, 2021). We calculated the filtered percent sand value for each sediment sample by subtracting a 7-point moving mean from the raw percent sand values (Fig. S5) downcore to eliminate the influence of decadal variations (spanning ~15 years) in local background sedimentation. We define event layers as filtered percent sand values that exceeded 95% of the cumulative distribution of the filtered percent sand data over the entire record. To account for differences in methodologies, and for a consistent comparison to the TC records from the Great Blue Hole (Schmitt et al., 2020) and Northeast Yucatan, we re-analyzed their percent sand data, defined event layers, and generated 100-yr frequencies following the same methods for our sediment cores.

2.2.2. Generating site-specific 100-yr TC frequencies

To analyze event frequency over the course of the Pelican Cays record, we created a composite record for the Pelican Cays using event layers from both ELB and LGN cores. The methods for creating this composite record were adapted from previous work by Wallace et al. (2019; 2021). To form the Pelican Cays composite record, we consolidated multiple events that fell within the ELB and LGN age model uncertainties (1σ) into single assumed TC strikes. When several events from one site fell within age model uncertainties of an event from another site, we only consolidate the event that is closest in median age to that of the event from the second site. For each event going into our composite, we sampled 1000 different age estimates from our Bacon age model. We used the age model from the core with the smallest age uncertainties for each event (Elbow Cay). Using our 1000 different age estimates, we built age probability distribution functions (pdfs) for each event in the Pelican Cays composite between 850 and 2000 CE. Each individual pdf sums to one and provides an estimate of the probability that each event happened in any given year. Since many of these events' age pdfs overlap, we summed all the overlapping age pdf values for Elbow Cay and Lagoon Cay. Following the same methods for the ELB and LGN sediment cores to create the Pelican Cays composite record, we created a site-specific composite record for the Northeast Yucatan by pulling two sediment cores from a nearby published record from Cenote Muyil, Lake Chunyaxche, Mexico (Sullivan et al., 2022). We were unable to create a site-specific composite record for the Great Blue Hole, Belize (Denommee et al., 2014; Schmitt et al., 2020) because we could not obtain uncalibrated original ^{14}C dates to generate a Bacon age model which is required for the compilation methodology. To define active and quiet TC intervals in the TC records, we calculated the mean and + 1σ and -1σ event frequency based on the 100-yr moving count, providing us with active and quiet intervals, respectively. We consider frequency counts occurring above the +1σ limit to be an active interval and frequency counts occurring below the -1σ limit to be a quiet interval and present these data as the moving *Z*-score for each respective record (Figs. 4c; 5e-h). Lastly, we determined the Pearson correlation coefficients between groups of records. The first group compared the individual ELB and LGN sediment records. The second group compared the Pelican Cays composite record, both re-analyzed Great Blue Hole records, and the re-analyzed Northeast Yucatan composite record.

3. Results

3.1. Age-depth models

Cores ELB and LGN each have mean sediment accumulation rates of 0.5 cm/yr for the entire core with mean initial and basal dates of 2007 CE and 810 CE for ELB (Fig. 2a), and 2007 CE and 730 CE for LGN (Fig. 2b). Peak ^{137}Cs accumulation in ELB occurred at a depth of 22.5 cm (Fig. 2a; Fig. S3) and 24.5 cm in LGN (Fig. 2b; Fig. S4). The absence of any outlier ^{14}C ages (falling outside the 95% confidence intervals; Fig. 2a, b) and visual bioturbation (i.e., blurred and wavy contacts between sediment layers and/or burrows and tunnels; Fig. S2) in the cores also supports the constant sediment accumulation rate.

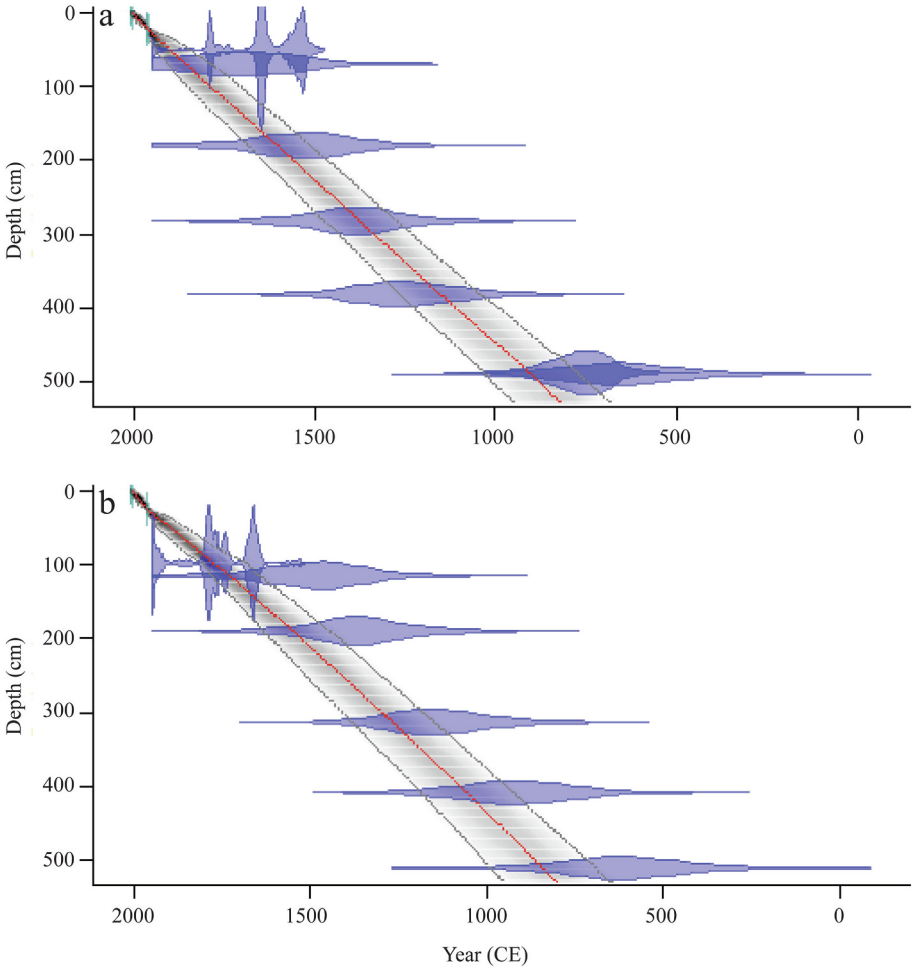

Fig. 2. Bacon age-depth models for (a) ELB and (b) LGN sediment cores. The 95% confidence interval is indicated by the grey dotted lines bracketing the age-depth shaded probability distribution curves. The weighted mean age-depth profile is indicated by the solid red line. Calibrated 2σ ^{14}C age distributions probabilities are shown in blue, and ages derived from ^{137}Cs calendar dates (1963 CE ±2) are shown as a green vertical bar. (For interpretation of the references to colour in this figure legend, the reader is referred to the web version of this article.)

3.2. Historic and full core grain size interpretation

During the historic period (1851–2007 CE), ELB recorded five event layers with mean ages of 1949 CE, 1919 CE, 1905 CE, 1889 CE, and 1870 CE, and LGN recorded seven event layers with mean ages of 1981 CE, 1972 CE, 1957 CE, 1935 CE, 1921 CE, 1912 CE, and 1890 CE that exceeded our event layer threshold (2.47% sand for ELB and 3.98% sand for LGN; Fig. 3a). Throughout the entire core (including the historic period), ELB recorded 22 event layers from 810-2007 CE and LGN recorded 23 event layers from 730-2007 CE (Fig. 3b, c).

3.3. 100-yr window event frequencies for the Pelican Cays and other nearby sites

3.3.1. Active and quiet TC intervals

The average 100-yr frequency for ELB and LGN is 1.9 ± 1.2 events/century and 1.5 ± 1.6 events/century, respectively (Fig. 4a). The ELB frequency record, presented as the moving *Z*-score, contains two active intervals during 1626–1631 CE and 1789–1938 CE, and two quiet intervals during 1059–1090 CE and 1277–1317 CE (Fig. S6). The LGN frequency record, presented as the moving Z-score, contains five (although two last <10 years) active intervals during 780–808 CE, 1501–1546 CE, 1701–1709 CE, 1794–1799 CE, and 1842–1957 CE and no quiet intervals (Fig. S6). Cores ELB and LGN had a correlation coefficient of 0.715 ($p < 0.00$).

In the Pelican Cays composite record, the average 100-yr frequency is 2.83 ± 2.27 events/century (Fig. 4b). The Pelican Cays frequency record, presented as the mean moving Z-score, contains one active interval from 1740-1950 CE and one quiet interval from 850-1018 CE (Fig. 5a). The Pelican Cays composite record had a correlation coefficient with the re-analyzed Great Blue Hole record (Schmitt et al., 2020) of −0.3661 ($p < 0.00$), the re-analyzed Great Blue Hole record (Denommee et al., 2014) of −0.6254 ($p < 0.00$), and the re-analyzed Northeast Yucatan composite record (Sullivan et al., 2022) of −0.5640 ($p < 0.00$).

In the re-analyzed Northeast Yucatan composite record (Sullivan et al., 2022), the average 100-yr frequency is 4.51 ± 2.57 events/century (Fig. 5b). The frequency record, presented as the mean moving Z-score, contains one active interval from 1234-1422 CE and two quiet intervals from 1484-1559 CE and from 1816-1853 CE (Fig. 5f). The re-analyzed Northeast Yucatan record had a correlation coefficient with the re-analyzed Great Blue Hole record (Schmitt et al., 2020) of 0.3797 ($p < 0.00$) and the re-analyzed Great Blue Hole record (Denommee et al., 2014) of 0.4317 ($p < 0.00$).

In the re-analyzed Great Blue Hole record (Denommee et al., 2014), the average 100-year frequency is 11.21 ± 5.58 events/century (Fig. 5c). The frequency record, presented as the moving Z-score, contains one active interval from 1421-1600 CE and two quiet intervals from 907-1046 CE and 1176–1208 CE (Fig. 5g). In the re-analyzed Great Blue Hole record (Schmitt et al., 2020), the average 100-year frequency

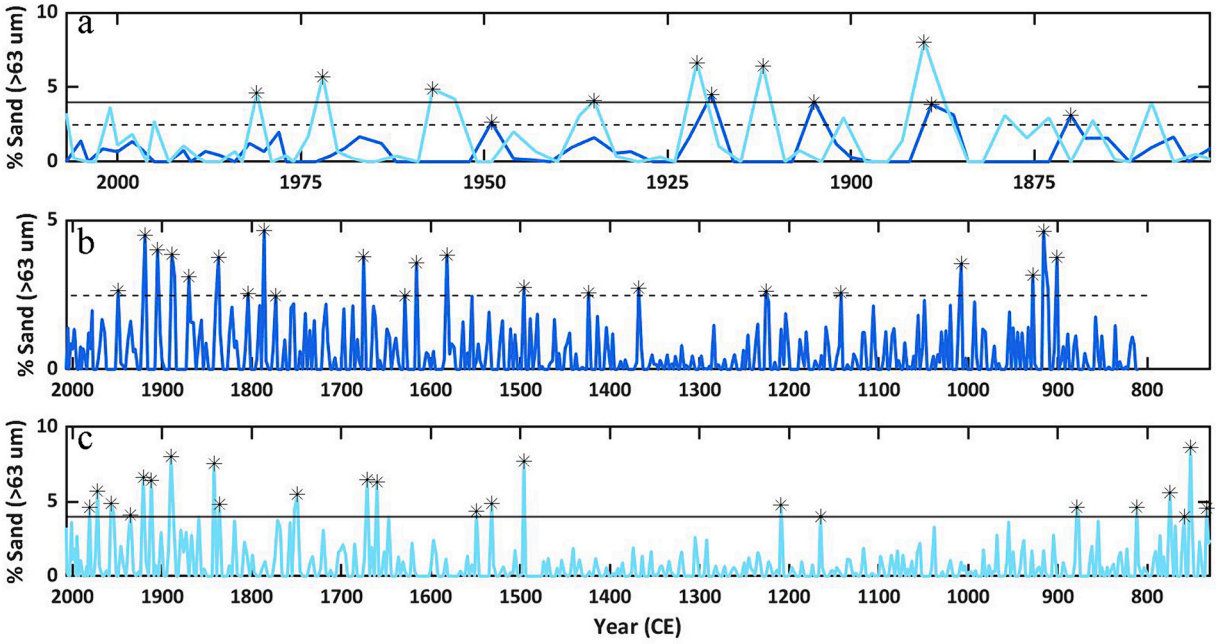

Fig. 3. (a) Filtered percent sand record during the historic period (1851–2007 CE) recorded in ELB (blue) and LGN (teal) sediment cores. Full core filtered percent sand record for (b) ELB and (c) LGN. Event layers are marked with black asterisk. The dashed line is the 95% threshold for ELB, and the solid line is the 95% threshold for LGN. (For interpretation of the references to colour in this figure legend, the reader is referred to the web version of this article.)

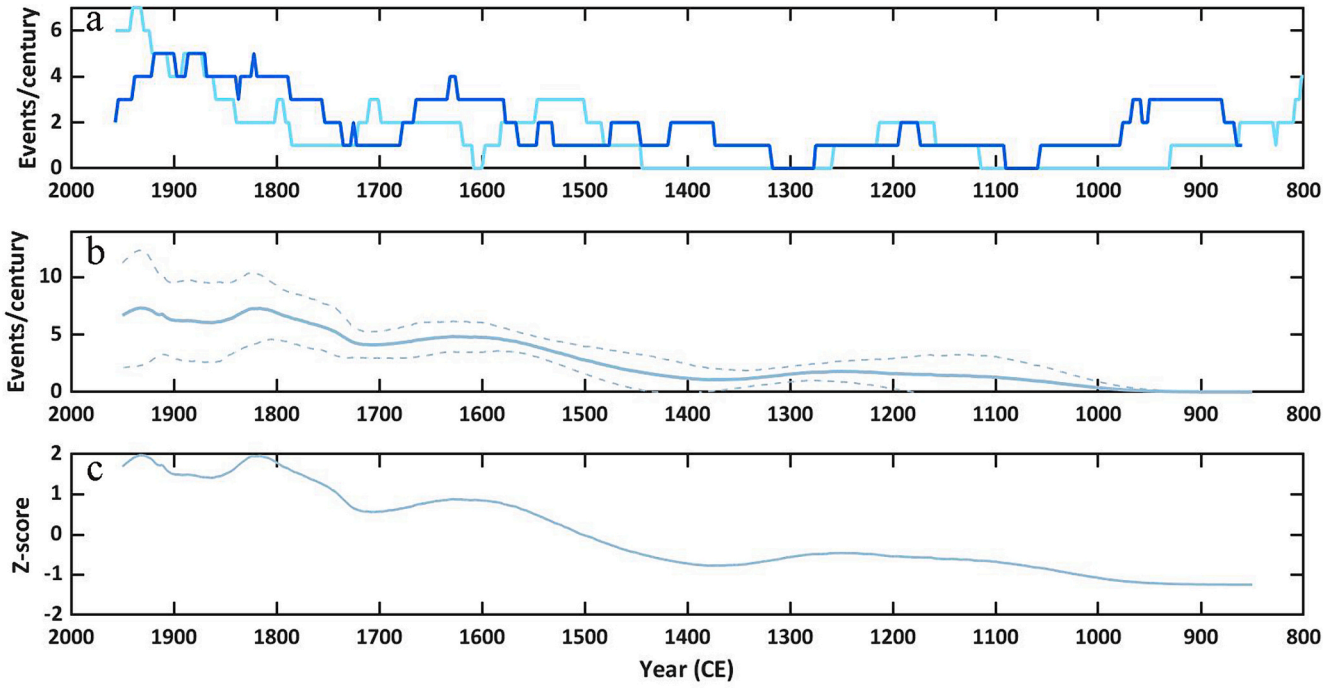

Fig. 4. (a) 100-yr frequency analysis for ELB (blue), LGN (teal) and (b) Pelican Cays composite record with the 95% confidence range represented by the dashed lines following the average 100-yr frequency (solid blue line). (c) Moving *Z*-score derived from the Pelican Cays composite frequency analysis. (For interpretation of the references to colour in this figure legend, the reader is referred to the web version of this article.)

is 3.74 ± 1.79 events/century (Fig. 5d). The frequency record, presented as the moving Z-score, contains two active intervals from 1099-1333 CE and 1434–1533 and one quiet interval from 1641-1802 CE (Fig. 5h). The re-analyzed Great Blue Hole records from Schmitt et al. (2020) and Denommee et al. (2014) had a correlation coefficient of 0.3692 ($p < 0.00$).

4. Discussion

4.1. Sediment core age models and interpreting modern events

Both the ELB and LGN cores exhibit stable and linear sediment accumulation rates of 0.5 cm/yr with no age reversals, outliers, nor visual evidence of bioturbation (Fig. S6). Homogeneous sedimentation in the ELB and LGN cores reflect the near-stable paleoenvironment/

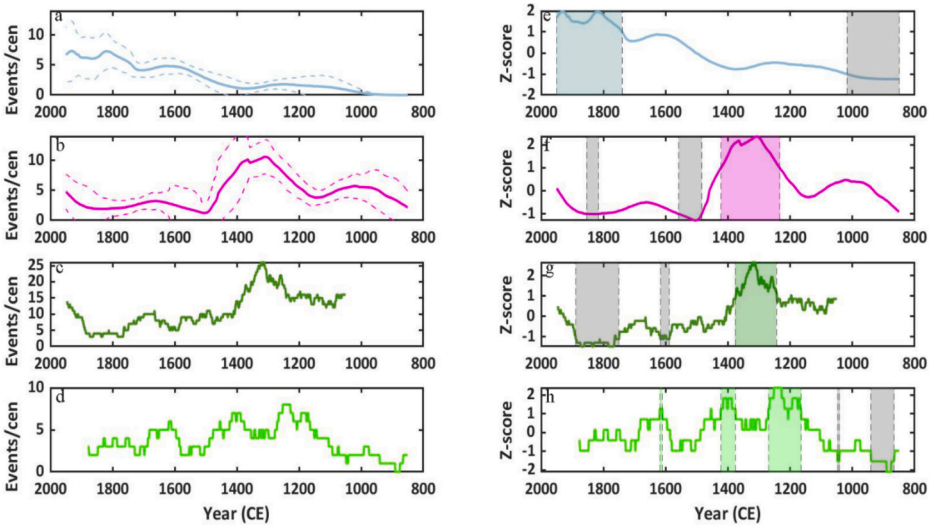

Fig. 5. (a) 100-yr frequency analysis for Pelican Cays composite record, (b) re-analyzed Northeast Yucatan composite record, (c) re-analyzed Great Blue Hole record (Denommee et al., 2014), and (d) re-analyzed Great Blue Hole record (Schmitt et al., 2020). (e-f) Moving Z-score derived from each respective 100-yr frequency analysis with colour-shaded regions indicating active intervals ($> +1\sigma$) and grey-shaded regions indicating quiet intervals ($< -1\sigma$). (For interpretation of the references to colour in this figure legend, the reader is referred to the web version of this article.)

relative sea level over the past 1000 years (Gischler and Hudson, 2004). The gas bench method for analyzing ^{14}C ages on bulk carbonate has larger age uncertainties than higher resolution traditional AMS dates on plant macrofossils and coral, rendering them less precise for age modeling (Fig. 2a, b; Table S1), especially in cores with high sedimentation rates. However, it is more cost effective (~2.5× less expensive) to use gas bench dates at higher density for age modeling purposes. In fact, recent research has shown that higher density and lower resolution dates are better than fewer higher resolution dates (Blaauw et al., 2018). Additional age uncertainty was added with the use of a marine reservoir correction of 157 years ±26 years from Glovers Reefs, Belize (~43 km to the northeast). The use of a marine reservoir correction from Glover's Reef, Belize was a conservative approach because of the abundance of older carbonate in the surrounding karst environment (Macintyre et al., 2000).

Historic event layers are of particular interest because they can serve as modern analogues, providing insight into types of storms conducive to producing event layers recorded in the Pelican Cays. In ELB, there are five event layers (four of which we could temporally correlate to historic $TCs_{100\ km}$) with mean ages of 1949 CE (TC 1945, Cat 1), 1919 CE (TC 1918, Cat 1), 1905 CE (TC 1906, Cat 1), 1889 CE (TC 1892, Cat 2), and 1870 CE (unassigned; Fig. 3a). The 1949 CE and 1919 CE event layers were produced by TCs that approached from the east and passed to the south of the Pelican Cays. The 1905 CE event layer was produced by a TC that approached from the south and passed to the east of the Pelican Cays. These directional setups are ideal for producing event layers, as the prevailing winds of the TC system generate the strongest waves toward the Pelican Cays.

Hypothetically, the relative position and direction of the 1892 Cat 2 were not ideal to generate wave conditions strong enough to produce the 1889 CE event layer (i.e., it approached from the east but was ~70 km to the north of the Pelican Cays). However, two scenarios could explain this: (1) A strong Cat 2 TC approaching from the east but passing ~70 km north of the Pelican Cays could pull water away from the Pelican Cays, via the prevailing southwesterly winds. Following the storm's passage, the rebound of coastal waters could produce a surge strong enough to breach the mangrove boundaries (such a phenomenon occurred recently in Tampa Bay, following the passage and landfall of Category 5 TC Ian); (2) The fetch between the Pelican Cays and Belize mainland (approximately 12 km) might have been sufficient for Category 2 TC-induced waves to generate significant waves, particularly with the inlet on the west side of Elbow Cay (Fig. 1d). However, 12 km of fetch is generally insufficient to produce large Category 2 TC-induced waves necessary to breach a mangrove-bounded cay, even with other conducive TC conditions. Longer fetches (at least 50–100 km) are typically required to generate wave heights associated with significant coastal impacts during TCs (MacAfee and Bowyer, 2005). In LGN, there are seven event layers that we could temporally correlate to historic TCs within 100 km, with mean ages of 1981 CE (Greta 1978, Cat 3), 1972 CE (Fifi 1974, Cat 2), 1957 CE (Hattie 1961, Cat 4; or Anna 1961, Cat 1; or Abby 1960, Cat 1), 1935 CE (TC 1931, Cat 4; or TC 1941, Cat 1), 1921 CE (TC 1918, Cat 1), 1912 CE (TC 1906, Cat 1), and 1890 CE (TC 1892, Cat 2). The 1972 CE and 1921 CE event layers were produced by Category 2 Fifi (1974 CE) and the 1918 CE Category 1 TC, respectively, both of which approached from the east and passed to the south of the Pelican Cays. The 1957 CE and 1935 CE event layers correlate with several possible historic TCs within 100 km. Regarding the 1957 CE event layer, TCs Anna and Abby had nearly identical paths, exemplifying ideal TC characteristics conducive to generating event layers (i.e., approaching from the east and passing ~10 km to the south of Pelican Cays). On the other hand, Hattie approached from the east and passed ~60 km to the north of the Pelican Cays (i.e., hypothetically unideal conditions for event layer generation). Confidence in event layer attribution would have been higher using storm surge and sediment transport models of historic storms, such as SLOSH (Glahn et al., 2009) or ADCIRC (Lin et al., 2014), but detailed bathymetry, which underpins the models' outputs, is lacking in this region. Without storm surge and sediment transport models of historic storms, we could only match event layers to historic storms based on the timing of deposition. Our attribution analysis indicates that event layer generation in the Pelican Cays is likely sensitive to all hurricanes within 100 km (Cat 1–5 TCs). Regarding the one unassigned event layer in ELB deposited in 1870 CE, it is possible a lesser magnitude storm wasn't documented, especially if it affected a less populated area (such as the Pelican Cays). Conversely, a major TC striking a heavily populated area like Belize City would have been documented, particularly before the established pre-instrumental period of 1785–1851 CE when British settlement and economic activities expanded (Friesner, 1993). A tsunami occurred in 1856 CE along the Honduran coast and was recorded in Belize (McCann and Pennington, 1990; O'Loughlin and Lander, 2003). This date closely matches the 1870 CE event layer recorded in ELB; thus, we cannot rule out the possibility of a tsunami-induced coarser grained deposit (discussed in

more detail in the next section). Nor can we entirely rule out the possibility of a tropical storm producing an event layer, especially when its proximity to the coring site is ideal. However, based on the ratio of historic tropical storms within 100 km of the Pelican Cays (17 between 1851 and 2007 CE) to event layers preserved in cores ELB (5) and LGN (7), and the presumption that tropical storms are too weak to produce event layers in this complex mangrove-bounded cay environment, we believe most event layers are from higher magnitude storms.

4.2. Tropical cyclone records and the suitability of the grain size proxy

The distribution of unfiltered total percent sand for cores ELB and LGN ranged from 0-60% sand (Fig. S4), while the distribution of filtered percent sand (with the 7-year running mean removed) ranged from 0-10.5% sand (Fig. 3a-c). The coarse anomaly values for ELB and LGN are lower than those from Bahama blue hole sediment cores (Wallace et al., 2019; Wallace et al., 2021a, 2021b; 0–50% sand) but similar to those from the Great Blue Hole sediment cores (Schmitt et al., 2020; 0–10% sand). Despite nuances in grain size statistics, TC frequency in cores ELB and LGN match well ($r = 0.715$; Fig. 4a, b). These results are novel, indicating that TC records from complex mangrove-bound cay environments, approximately 8 km apart, can be correlated.

Despite the relatively fast mean sedimentation rates of Elbow Cay (0.5 cm/yr) and Lagoon Cay (0.5 cm/yr), we found that Elbow Cay and Lagoon Cay do not record as many event layers (22 in ELB and 23 in LGN) as other nearby sites studied in paleotempestology, such as the Great Blue Hole (150 event layers in 1200 years, Denommee et al., 2014; 157 event layers in 1885 years, Schmitt et al., 2020). One explanation for the lower number of recorded event layers in ELB and LGN could be the comparatively lower number of TCs that track toward south of the Great Blue Hole, striking the Pelican Cays. A more likely explanation is that Elbow Cay and Lagoon Cay are not as sensitive to TC-generated waves, considering the complex mangrove-bounded cay environment surrounding the Elbow and Lagoon Cay, and their proximity to the Great Blue Hole (~100 km; Fig. 1). The latter explanation would have been investigated further if it were not for the lack of high-resolution bathymetric data in the region, precluding us from running accurate storm-induced wave models.

Although the ELB and LGN records generally agree, they only share three event layers produced by historic TCs: 1918 CE (Cat 1), 1906 CE (Cat 1), and 1892 CE (Cat 2; Fig. 3a). Interestingly, LGN recorded only one more event layer in the entire record despite being 27 cm longer and approximately 80 years older (Fig. 3a-c). This discrepancy in event layer generation is most likely due to site-specific differences in grain size distributions and site geomorphology. For example, both cays are surrounded by other cays of varying size, shape, elevation, and ecologies (i.e., presence of red mangroves). Elbow Cay's fringing mangroves are widest on its southern end, spanning about 140 m, while Lagoon Cay's fringing mangroves are widest on its western side, spanning about 90 m (Fig. 1c, d). Elbow Cay's thicker mangrove growth on the south side might partially explain why it is less sensitive to event layer generation in the historic period, considering the majority of TCs approach from the southeast (Fig. 1a). Additionally, Elbow Cay has a secondary (and smaller) lagoon that would theoretically be impacted by storm-induced waves before the primary (and larger) lagoon where we cored (Fig. 1d). If this were the case, we would expect storm-induced sediments to fall out of suspension and deposit in the smaller lagoon before reaching the larger lagoon, thereby not being recorded by the ELB core or not recorded in the same way as LGN.

Depending on individual TC characteristics (storm track, angle of approach, size, and relative strength), surrounding cays could provide allochthonous coarser-grained sediment to get deposited in the depocenters of either one or both cays. Conversely, these surrounding cays could inhibit sediment transport by blocking the strongest waves and surge responsible for sediment transport. Additionally, both Elbow Cay and Lagoon Cay have inlets; Elbow Cay's western inlet was anthropogenically dredged between 2006 and 2010 CE, while Lagoon Cay's southern inlet has remained the same throughout the satellite era (1969 CE-present; Google Earth). Considering the topmost mean ages of the ELB and LGN cores were both 2007 CE, there is little impact of inlet dredging on the current sediment records. Lagoon Cay's southern inlet might provide easier access for sediment to get transported into the lagoon's depocenter, especially when a majority of Belizean landfalling TCs come from the southeast (Fig. 1a).

There is a limited possibility of tsunami-driven deposition into the cays, potentially mimicking TC deposits in terms of percent sand. Belize lies north of the junction where the North American plate subducts beneath the Caribbean plate; however, near Belize, this junction occurs as a strike-slip fault, resulting in predominantly lateral plate movement (Donnelly et al., 1990). This lateral plate movement reduces the likelihood of local tsunami generation. Furthermore, the likelihood of far-field tsunami generation originating in the Antillean Island Arc is low and small (Scheffers et al., 2005). In fact, only three tsunamis generated along the Honduran coast have been recorded near Belize since 1498 CE: in 1856 CE, 1797 CE, and 1539 CE (McCann and Pennington, 1990; O'loughlin and Lander, 2003). The 1856 CE and 1539 CE tsunamis are closely correlated with the mean age of event layers in both ELB and LGN cores. In ELB, one event layer was deposited in 1870 CE, and in LGN, two event layers were deposited in 1842 CE and 1532 CE. Unfortunately, we cannot statistically or visually distinguish between potential tsunami- and TC-induced coarser-grained deposits in either ELB or LGN. However, considering the ratio of tsunamis to TCs during the historic period (i.e., no tsunamis occurred between 1851-2007 CE), we suggest that most event layers are indeed produced by TCs. In addition to tsunami-driven deposition, seismic events triggering turbidites and potentially high-energy waves could transport coarser-grained sediments into the depocenters of the lagoons. For example, a 7.5-magnitude earthquake near the Swan Islands in 2004 (~450 km northeast of the Pelican Cays) produced an event layer in the Great Blue Hole record by triggering instabilities on the interior sediment slope, causing turbidites to re-deposit sediment at the bottom of the blue hole (Schmitt et al., 2020). Additionally, the United States Geological Survey suggests a 7.5-magnitude earthquake return period of once per 150 years (Schmitt et al., 2020), which when extrapolated over the ELB and LGN event layer sediment records, suggests that approximately eight event layers could have been generated by seismic events (25–36% of events recorded). We argue that earthquake-induced event layers are likely not the cause of event layers in Elbow Cay and Lagoon Cay because they are small (north-to-south lagoon diameters of ~400–500 m), with much shallower basins (~15 m), and lack sediment-laden slopes sufficient to feed intra-basin turbidity flows (Fig. S1). Lastly, the entire Caribbean experiences major earthquakes 10–100 times less frequently than TC landfalls (Lander et al., 2003), and therefore the ratio between Caribbean TC landfalls and earthquake occurrences indicates that these event layers were more likely produced by TCs.

4.3. Comparison between the Pelican Cays composite record, Northeast Yucatan composite record, and the Great Blue Hole records

The high-resolution (0.5 cm/yr) Pelican Cays composite record is useful for comparison with re-analyzed records from the Great Blue Hole (Denommee et al., 2014; Schmitt et al., 2020) and Cenote Muyil, Northeast Yucatan (Sullivan et al., 2022) within an overlapping time window from 1000-2000 CE (Fig. 5a-c). Generally, throughout the entirety of the records, we found that the Pelican Cays composite record is significantly ($p < 0.00$) anticorrelated with both re-analyzed Great Blue Hole records ($r = -0.62$, Denommee et al., 2014; $r = -0.36$, Schmitt et al., 2020) and the Northeast Yucatan record ($r = -0.56$; Sullivan et al., 2022). The anticorrelation, especially between the Pelican Cays and Northeast Yucatan, is not surprising considering that the two sites are never experiencing the same TC_{100km} ($\geq$ Category 2) during the historic period (1851–2007 CE; Fig. 1a). The anticorrelation between

the Pelican Cays and Great Blue Hole is more surprising considering these sites do share five TC_{100km} (≥ Category 2) during the historic period (1851–2007 CE; Fig. 1a). The first antiphase (Antiphase I) occurs from 1740-1920 CE, when the Pelican Cays composite record has an average positive *Z*-score of 1.56, ranging from 1.00 to 1.96. Meanwhile, the Great Blue Hole record (Denommee et al., 2014) has an average negative Z-score of −1.32, ranging from −1.47 to −0.22; the Great Blue Hole record (Schmitt et al., 2020) has an average negative Z-score of −0.40, ranging from −0.97 to 0.14; and the Northeast Yucatan composite record (Sullivan et al., 2022) has an average negative Z-score of −1.00, ranging from −1.01 to −0.51. The second antiphase (Antiphase II) occurs from 1200-1400 CE, when the Pelican Cays composite record has an average negative Z-score of −0.60, ranging from −0.46 to −0.78. In contrast, the Great Blue Hole record (Denommee et al., 2014) has an average positive Z-score of 1.37, ranging from 0.14 to 2.65; the Great Blue Hole record (Schmitt et al., 2020) has an average positive Z-score of 1.05, ranging from 0.14 to 2.37; and the Northeast Yucatan composite record has a positive Z-score of 1.71, ranging from 0.38 to 2.35.

Past studies have relied on using a single TC record to infer climate impacts on TC activity over the past few thousand years (Denommee et al., 2014; van Hengstum et al., 2014, 2016; Wallace et al., 2019; Schmitt et al., 2020; Winkler et al., 2020). Wallace et al. (2021) suggest that individual records likely suffer from sampling bias and that cores from individual sites likely capture a small subset of TCs moving through the Caribbean, especially in the Bahamas (Wallace et al., 2021). Thus, such climate inferences are difficult to support when only one core is assumed to represent TC activity over a broad geographic region. Considering the proximity of the Pelican Cays and Great Blue Hole (~100 km) and their inversely correlated records, we suggest that the observed anticorrelation between these two sites is likely due to randomness, especially when these sites are most likely experiencing the same broad regional climate signal, while simultaneously affected by noisy local ocean-air dynamics. These dynamics include complex interactions between the El Niño-Southern Oscillation and the Madden-Julian Oscillation, which serve to modulate the CLLJ by intensifying it and prolonging its life cycle (Martinez et al., 2020). In fact, Wallace et al. (2021) show that the climate signal is significant between Bahama sites over 400 km apart (Wallace et al., 2021), and our sites all lie within 400 km of each other. On the other hand, there are not enough studies for us to confidently assume that climate over the past millennium had absolutely no control over variability between the Pelican Cays, Great Blue Hole, and Northeast Yucatan. To help explain the evident anticorrelation between western Caribbean sites, integrating more existing TC records and conducting TC model runs over the past millennium to assess the significance of centennial-scale variability in TC activity recorded in reconstructions is needed.

4.4. Long-term asynchrony in North Atlantic TC frequency from 1200-1800 CE

4.4.1. First period of asynchrony: 1200–1400 CE

When we consider the records from this study and other high-resolution TC composite or individual records from the Florida Gulf Coast (Wallace et al., 2021a, 2021b), New England (Wallace et al., 2021a, 2021b), Bahamas Archipelago (Wallace et al., 2021a, 2021b), and Puerto Rico (Donnelly and Woodruff, 2007), we find increasing evidence of asynchrony in TC patterns across the North Atlantic basin beginning around 1200 CE and lasting until 1400 CE, supporting the hypothesis from previous studies (Wallace et al., 2021a, 2021b). During this period, both the Bahama Archipelago composite and New England composite records indicate a lower TC frequency, while both the Northeast Yucatan composite and re-analyzed Great Blue Hole records document the most extreme TC frequency compared to any other time during the last millennium (1000–2000 CE; Fig. 5b, c, d). Interestingly, the Pelican Cays composite record does not capture this increase in western Caribbean TC frequency (Fig. 5a). Thus, we suggest that the evident reduction in TC frequency documented in the Pelican Cays composite record could be a randomly driven local signal in TC activity, and not a climate-driven regional signal. For example, instantaneous stochastic variability occurring in daily ocean-atmosphere dynamics could have been more conducive to shifting TCs, already heading toward Belize, slightly north of the Pelican Cays, and striking the Great Blue Hole and Northeast Yucatan.

4.4.2. Second period of asynchrony: 1400–1700 CE

During the Little Ice Age (LIA: 1400–1700; Mann et al., 2009), the Bahama Archipelago composite and New England composite records (Wallace et al., 2021a, 2021b) show increased TC frequency, coeval to a time when the Northeast Yucatan composite record, re-analyzed Great Blue Hole records, Florida Gulf Coast composite record (Wallace et al., 2021a, 2021b), and Laguna Play Grande, Vieques, Puerto Rico record (Donnelly and Woodruff, 2007) all document a reduction in TC frequency. Unlike the substantial decreasing trend in TC frequency from these western Caribbean and Florida Gulf Coast records, the Pelican Cays composite record shows a rise in TC frequency (although this rise is not statistically significant; Fig. 5). Again, we attribute this increase to a randomly driven local signal in TC activity. Although the Pelican Cays composite record is not capturing the same climate-driven reduction in TC strikes as other TC records, Atlantic Multidecadal Variability (AMV) reconstructions for the past millennium (Mann et al., 2009; Wang et al., 2017) indicate a persistently negative phase during the LIA, particularly during the 15th-century onset. We know from Kossin (2017) that SSTs of the TC main development region (9° N to 20° N, running longitudinally along the northern edge of the Intertropical Convergence Zone) co-vary inversely with vertical wind shear (VWS), indicating that during periods of decreased SSTs (as seen during the LIA), we can expect higher levels of VWS. This increase in VWS resulting from the persistently negative AMV could have prevented TCs from intensifying before they made landfall in the western Caribbean, Puerto Rico, and along the Gulf Coast of Florida. Additionally, this shift in the 1400s toward more TCs striking along the U.S. East Coast and Bahamas and fewer TCs striking in the western Caribbean and Gulf could also signify a transition toward more recurving storm tracks hypothetically linked to a northeastward shift in the mid-latitude jet and NASH. We cannot directly test this hypothesis due to the paucity of paleo-reconstructions for either the NASH or North Atlantic mid-latitude. However, previous studies have shown a weakening (displacement toward the northeast) of the NASH in a colder climate (Li et al., 2012; Colbert and Soden, 2012), supporting the observed asynchrony in the North Atlantic TC records during the LIA.

4.5. Potential shift from North Atlantic TC asynchrony to synchrony: 1900 CE-Present?

Starting in 1900 CE, the Pelican Cays composite, Northeast Yucatan composite, Great Blue Hole, New England composite, and Puerto Rico records all document increased TC frequency, except for the Bahamas Archipelago composite record (Wallace et al., 2021a, 2021b), which experienced a substantial reduction in storm activity during the past 200 years compared to any other time over the last millennium. This suggests overall synchrony in TC activity in the North Atlantic basin. Explaining this observed basin-wide increase is difficult, especially when synchronous TC activity coincides with competing climate factors that should lead to TC asynchrony amid a warming climate. For example, with anthropogenic warming, we should expect this pattern of increased TC frequency for the U.S. East Coast to continue because with the predicted future expansion of the Hadley cell (Lu et al., 2007; Kang and Lu, 2012) and warmer SSTs expanding into the subtropical North Atlantic (Ting et al., 2015), powerful TCs are projected to make landfall more often along the U.S. East Coast (Ting et al., 2019). Additionally, with warming SSTs, especially in the main development region, we can expect decreased VWS, further favoring basin-wide TC conditions. However, one competing factor is the presumed strengthening

(southwest expansion) of the NASH, which would likely steer more TCs toward the western Caribbean and Gulf of Mexico, effectively decreasing the number of TC strikes along the U.S. East Coast and Bahamas. Further complicating the TC-climate relationship is the Interdecadal Pacific Oscillation, a climate phenomenon characterized by long-term SST variations in the Pacific Ocean, typically on the scale of 15–30 years. It is comparable to the El Niño-Southern Oscillation but operates over a much longer timescale. A negative (La-Niña-like) cooler phase contributes to favorable TC conditions (Yang et al., 2024). Over the past millennium, we observed higher North Atlantic TCs during warmer main development region SSTs, thus hypothetically lower VWS, and a cooler phase of the Interdecadal Pacific Oscillation (La-Niña-like conditions).

5. Conclusions

In this study, we present a high-resolution tropical cyclone (TC) reconstruction over the past 1200 years from the most southern paleotempestological study site in Belize to date: Elbow Cay and Lagoon Cay, two reef-enclosed lagoons in the Pelican Cays, Belize. Our findings indicate that the sediment depositional environments of Elbow Cay and Lagoon Cay are likely recording TC-generated event layers from historic TCs within 100 km (1851–2007 CE; $\geq$ Category 1). Our TC frequency analysis indicates that the Pelican Cays composite record contains one active interval of increased TC activity from 1740-1950 CE and one quiet interval of decreased TC activity from 850-1018 CE. A comparison between the Pelican Cays composite record and re-analyzed Northeast Yucatan composite record and re-analyzed Great Blue Hole records reveals two periods of anticorrelated TC activity in the western Caribbean (Antiphase I and Antiphase II). During Antiphase I (1200–1400 CE), the re-analyzed Great Blue Hole records and Northeast Yucatan composite records indicate a dramatic increase in TC activity, while the Pelican Cays composite record shows a decrease. During Antiphase II (1740–1920 CE), TC activity in the Pelican Cays increases, coinciding with a decrease in TC frequency for the Great Blue Hole and Northeast Yucatan. We attribute these antiphases to randomness, although we cannot entirely rule out the possibility that a combination of climate forcings are indeed steering TCs, already heading toward Belize, either more south, hitting the Pelican Cays, or more north, hitting the Great Blue Hole and Northeast Yucatan.

Funding

Funding was provided to J. Donnelly by the Inter-American Institute for Global Change Research (IAI) and the National Science Foundation (Award 1903616).

CRediT authorship contribution statement

Chris L. Blanco: Conceptualization, Data curation, Formal analysis, Visualization, Writing – original draft, Writing – review & editing. **Andrea D. Hawkes:** Funding acquisition, Project administration, Supervision, Validation. **Elizabeth J. Wallace:** Methodology, Validation. **Jeffrey P. Donnelly:** Funding acquisition, Supervision. **Dana MacDonald:** Validation.

Declaration of competing interest

All authors declare no competing interests.

Data availability

Data will be available at Woods Hole Oceanographic Institution's Paleohurrdat repository (https://www2.whoi.edu/site/coastalgroup/paleohurrdat/).

Acknowledgments

We would like to thank former WHOI lab technicians Sam Zipper and *Skye* Moret-Ferguson for their assistance in the field. We also thank Lincoln Westby and Ransom Nunez from Tarpon Caye Lodge for all their great work and hospitality.

Appendix A. Supplementary data

Supplementary data to this article can be found online at https://doi.org/10.1016/j.margeo.2024.107365.

References

Adomat, F., Gischler, E., 2016. Assessing the suitability of Holocene environments along the Central Belize Coast, Central America, for the reconstruction of Hurricane Records. Int. J. Earth Sci. 106 (1), 283–309. https://doi.org/10.1007/s00531-016-1319-y.

Anderson, W.B., Seager, R., Baethgen, W., Cane, M., You, L., 2019. Synchronous crop failures and climate-forced production variability. Sci. Adv. 5 (7), eaaw1976.

Avila, L., 2001. Tropical Cyclone Report: Hurricane Iris, 4-9 October 2001. *National Hurricane Center* (issue October).

Beven, J., Berg, R., Hagen, A., 2019. Hurricane Michael (AL142018). In: *National Hurricane Center Tropical Cyclone* Report (issue May).

Blaauw, M., Christen, J.A., 2011. Flexible paleoclimate age-depth models using an autoregressive gamma process. Bayesian Anal. 6 (3) https://doi.org/10.1214/11-ba618.

Blaauw, M., Christen, J.A., 2013. Bacon Manual – V2.3.9.1.

Blaauw, M., Christen, J.A., Bennett, K.D., Reimer, P.J., 2018. Double the dates and go for Bayes — impacts of model choice, dating density and quality on chronologies. Quat. Sci. Rev. 188, 58–66. https://doi.org/10.1016/j.quascirev.2018.03.032.

Brouwer, R., Akter, S., Brander, L., Haque, E., 2007. Socioeconomic vulnerability and adaptation to environmental risk: a case study of climate change and flooding in Bangladesh. Risk Anal. 27 (2), 313–326. https://doi.org/10.1111/j.1539-6924.2007.00884.x.

Colbert, A.J., Soden, B.J., 2012. Climatological variations in North Atlantic tropical cyclone tracks. J. Clim. 25 (2), 657–673.

Denommee, K.C., Bentley, S.J., Droxler, A.W., 2014. Climatic controls on Hurricane patterns: a 1200-y near-annual record from Lighthouse Reef, Belize. Sci. Rep. 4 (1) https://doi.org/10.1038/srep03876.

Donnelly, J.P., Woodruff, J.D., 2007. Intense hurricane activity over the past 5,000 years controlled by El Niño and the West African Monsoon. Nature 447 (7143), 465–468. https://doi.org/10.1038/nature05834.

Donnelly, T.W., Home, G.S., Finch, R.C., López-Ramos, E., 1990. Northern Central America; the Maya and Chortis Blockse. The Caribbean Region, pp. 37–76. https://doi.org/10.1130/dnag-gna-h.37.

Donnelly, J.P., Hawkes, A.D., Lane, P., MacDonald, D., Shuman, B.N., Toomey, M.R., van Hengstum, P.J., Woodruff, J.D., 2015. Climate forcing of unprecedented intense-hurricane activity in the last 2000 years. Earth's Future 3 (2), 49–65. https://doi.org/10.1002/2014ef000274.

Druffel, E.M., 1980. Radiocarbon in annual coral rings of Belize and Florida. Radiocarbon 22 (2), 363–371. https://doi.org/10.1017/s0033822200009656.

Frappier, A.B., Sahagian, D., Carpenter, S.J., González, L.A., Frappier, B.R., 2007. Stalagmite stable isotope record of recent tropical cyclone events. Geology 35 (2), 111–114.

Friesner, J., 1993. Hurricanes and the Forests of Belize. Forest Department. Ministry of Natural Resources and the Environment, Belmopan City, Belize.

Gischler, E., Hudson, J.H., 2004. Holocene development of the Belize Barrier Reef. Sediment. Geol. 164 (3–4), 223–236. https://doi.org/10.1016/j.sedgeo.2003.10.006.

Gischler, E., Shinn, E.A., Oschmann, W., Fiebig, J., Buster, N.A., 2008. A 1500-year Holocene Caribbean climate Archive from the Blue Hole, Lighthouse Reef, Belize. J. Coast. Res. 246, 1495–1505. https://doi.org/10.2112/07-0891.1.

Gischler, E., Anselmetti, F.S., Shinn, E.A., 2013. Seismic stratigraphy of the Blue Hole (lighthouse reef, Belize), a late holocene climate and storm Archive. Mar. Geol. 344, 155–162. https://doi.org/10.1016/j.margeo.2013.07.013.

Glahn, B., Taylor, A., Kurkowski, N., Shaffer, W.A., 2009. The role of the SLOSH model in National Weather Service storm surge forecasting. Natl. Weather Digest 33 (1), 3–14.

Heaton, T.J., Köhler, P., Butzin, M., Bard, E., Reimer, R.W., Austin, W.E., Skinner, L.C., 2020. Marine20—the marine radiocarbon age calibration curve (0–55,000 cal BP). Radiocarbon 62 (4), 779–820.

Imbach, P., Chou, S.C., Lyra, A., Rodrigues, D., Rodriguez, D., Latinovic, D., Georgiou, S., 2018. Future climate change scenarios in Central America at high spatial resolution. PLoS One 13 (4), e0193570.

Kang, S.M., Lu, J., 2012. Expansion of the Hadley cell under global warming: Winter versus summer. J. Clim. 25 (24), 8387–8393.

Key, C.J., 2002. The political economy of the transition from fishing to tourism, in Placencia, Belize. Int. Rev. Mod. Sociol. 1–18.

Kishore, N., Marqués, D., Mahmud, A., Kiang, M.V., Rodriguez, I., Fuller, A., et al., 2018. Mortality in Puerto Rico after hurricane maria. N. Engl. J. Med. 379 (2), 162–170.

Knapp, K.R., Kruk, M.C., Levinson, D.H., Diamond, H.J., Neumann, C.J., 2010. The international best track archive for climate stewardship (IBTrACS) unifying tropical cyclone data. Bull. Am. Meteorol. Soc. 91 (3), 363–376.
Knutson, T., Landsea, C., Emanuel, K., 2010. Tropical cyclones and climate change: a review. In: World Scientific Series on Asia-Pacific Weather and Climate, pp. 243–284. https://doi.org/10.1142/9789814293488_0009.
Knutson, T., Camargo, S.J., Chan, J.C., Emanuel, K., Ho, C.-H., Kossin, J., Mohapatra, M., Satoh, M., Sugi, M., Walsh, K., Wu, L., 2020. Tropical cyclones and climate change assessment: Part II: projected response to anthropogenic warming. Bull. Am. Meteorol. Soc. 101 (3) https://doi.org/10.1175/bams-d-18-0194.1.
Kossin, J.P., 2017. Hurricane intensification along United States Coast suppressed during active Hurricane periods. Nature 541 (7637), 390–393. https://doi.org/10.1038/nature20783.
Lander, J.F., Whiteside, L.S., Lockridge, P.A., 2003. Two decades of global tsunamis. Sci. Tsunami Haz. 21 (1), 3.
Landsea, C.W., Glenn, D.A., Bredemeyer, W., Chenoweth, M., Ellis, R., Gamache, J., Hufstetler, L., Mock, C., Perez, R., Prieto, R., Sánchez-Sesma, J., Thomas, D., Woolcock, L., 2008. A reanalysis of the 1911–20 Atlantic hurricane database. J. Clim. 21 (10), 2138–2168. https://doi.org/10.1175/2007jcli1119.1.
Li, W., Li, L., Ting, M., Liu, Y., 2012. Intensification of Northern Hemisphere subtropical highs in a warming climate. Nat. Geosci. 5 (11), 830–834.
Lin, N., Lane, P., Emanuel, K.A., Sullivan, R.M., Donnelly, J.P., 2014. Heightened hurricane surge risk in Northwest Florida revealed from climatological-hydrodynamic modeling and Paleorecord Reconstruction. J. Geophys. Res. Atmos. 119 (14), 8606–8623. https://doi.org/10.1002/2014jd021584.
Lu, J., Vecchi, G.A., Reichler, T., 2007. Expansion of the Hadley cell under global warming. Geophys. Res. Lett. 34 (6).
MacAfee, A.W., Bowyer, P.J., 2005. The modeling of trapped-fetch waves with tropical cyclones—a desktop operational model. Weather Forecast. 20 (3), 245–263.
Macintyre, I.G., Precht, W.F., Aronson, R.B., 2000. Origin of the pelican cays ponds, Belize. Atoll Res. Bull. 466, 1–11. https://doi.org/10.5479/si.00775630.466.1.
Macintyre, I.G., Toscano, M.A., Feller, I.C., Faust, M.A., 2009. Decimating mangrove forests for commercial development in the Pelican Cays, Belize: long-term ecological loss for short-term gain? Smithson. Contrib. Mar. Sci. 38, 281–290.
Mann, M.E., Zhang, Z., Rutherford, S., Bradley, R.S., Hughes, M.K., Shindell, D., Ni, F., 2009. Global signatures and dynamical origins of the Little Ice Age and medieval climate Anomaly. science 326 (5957), 1256–1260.
Martinez, J.A., Arias, P.A., Castro, C., Chang, H.I., Ochoa-Moya, C.A., 2019. Sea surface temperature-related response of precipitation in northern South America according to a WRF multi-decadal simulation. Int. J. Climatol. 39 (4), 2136–2155.
Martinez, C., Kushnir, Y., Goddard, L., Ting, M., 2020. Interannual variability of the early and late-rainy seasons in the Caribbean. Clim. Dyn. 55 (5), 1563–1583.
McCann, W.R., Pennington, W.D., 1990. Seismicity, Large Earthquakes, and the Margin of the Caribbean Plate. The Caribbean Region, pp. 291–306. https://doi.org/10.1130/dnag-gna-h.291.
McCloskey, T.A., Keller, G., 2009. 5000-year sedimentary record of hurricane strikes on the Central Coast of Belize. Quat. Int. 195 (1–2), 53–68. https://doi.org/10.1016/j.quaint.2008.03.003.
McCloskey, T.A., Liu, K.-biu., 2012. A 7000-year record of Paleohurricane activity from a coastal wetland in Belize. The Holocene 23 (2), 278–291. https://doi.org/10.1177/0959683612460782.
Nancoo, M.E., 1962. Hurricane 'Hattie'. Weather 17 (9), 295–304. https://doi.org/10.1002/j.1477-8696.1962.tb07316.x.
Obrist-Farner, J., Steinman, B.A., Stansell, N.D., Maurer, J., 2023. Incoherency in central American hydroclimate proxy records spanning the last millennium. Paleoceanogr. Paleoclimatol. 38 (3) (e2022PA004445).
O'loughlin, K.F., Lander, J.F., 2003. About the 500-year tsunami history. Caribbean Tsunamis 19–35. https://doi.org/10.1007/978-94-017-0321-5_3.
Pollock, A.L., van Beynen, P.E., DeLong, K.L., Polyak, V., Asmerom, Y., Reeder, P.P., 2016. A mid-Holocene paleoprecipitation record from Belize. Palaeogeogr. Palaeoclimatol. Palaeoecol. 463, 103–111.
Reimer, P.J., Austin, W.E., Bard, E., Bayliss, A., Blackwell, P.G., Ramsey, C.B., Talamo, S., 2020. The IntCal20 Northern Hemisphere radiocarbon age calibration curve (0–55 cal kBP). Radiocarbon 62 (4), 725–757.
Scheffers, A., Scheffers, S., Kelletat, D., 2005. Paleo-tsunami relics on the southern and Central Antillean Island arc. J. Coast. Res. 212, 263–273. https://doi.org/10.2112/03-0144.1.
Schmitt, D., Gischler, E., Anselmetti, F.S., Vogel, H., 2020. Caribbean cyclone activity: an annually-resolved common era record. Sci. Rep. 10 (1) https://doi.org/10.1038/s41598-020-68633-8.
Stewart, S., Berg, R., 2018. Hurricane Florence (AL062018). In: National Hurricane Center Tropical Cyclone Report (issue September).
Sullivan, R.M., van Hengstum, Donnelly, J.P., Tamalavage, A.E., Winkler, T.S., Little, S. N., Korty, R., 2022. Northeast Yucatan hurricane activity during the Maya Classic and Postclassic periods. Sci. Rep. 12 (1), 20107.
Ting, M., Camargo, S.J., Li, C., Kushnir, Y., 2015. Natural and forced North Atlantic hurricane potential intensity change in CMIP5 models. J. Clim. 28 (10), 3926–3942.
Ting, M., Kossin, J.P., Camargo, S.J., Li, C., 2019. Past and future hurricane intensity change along the US East Coast. Sci. Rep. 9 (1), 7795.
van Hengstum, Donnelly, J.P., Fall, P.L., Toomey, M.R., Albury, N.A., Kakuk, B., 2016. The intertropical convergence zone modulates intense hurricane strikes on the western North Atlantic margin. Sci. Rep. 6 (1), 21728.
van Hengstum, P.J., Donnelly, J.P., Toomey, M.R., Albury, N.A., Lane, P., Kakuk, B., 2014. Heightened hurricane activity on the Little Bahama Bank from 1350 to 1650 AD. Cont. Shelf Res. 86, 103–115.
Wallace, E.J., Coats, S., Emanuel, K., Donnelly, J.P., 2021. Centennial-scale shifts in storm frequency captured in paleohurricane records from The Bahamas arise predominantly from random variability. Geophys. Res. Lett. 48 (1), e2020GL091145.
Wallace, E.J., Donnelly, J.P., Hengstum, P.J., Wiman, C., Sullivan, R.M., Winkler, T.S., d'Entremont, N.E., Toomey, M., Albury, N., 2019. Intense hurricane activity over the past 1500 years at South Andros Island, the Bahamas. Paleoceanogr. Paleoclimatol. 34 (11), 1761–1783. https://doi.org/10.1029/2019pa003665.
Wallace, E., Donnelly, J., van Hengstum, P., Winkler, T., Dizon, C., LaBella, A., Lopez, I., d'Entremont, N., Sullivan, R., Woodruff, J., Hawkes, A., Maio, C., 2021a. Regional shifts in paleohurricane activity over the last 1500 years derived from blue hole sediments offshore of Middle Caicos Island. Quat. Sci. Rev. 268, 107126 https://doi.org/10.1016/j.quascirev.2021.107126.
Wallace, E.J., Donnelly, J.P., van Hengstum, P.J., Winkler, T.S., McKeon, K., MacDonald, D., d'Entremont, N.E., Sullivan, R.M., Woodruff, J.D., Hawkes, A.D., Maio, C., 2021b. 1,050 years of hurricane strikes on Long Island in the Bahamas. Paleoceanogr. Paleoclimatol. 36 (3) https://doi.org/10.1029/2020pa004156.
Wang, J., Yang, B., Ljungqvist, F.C., Luterbacher, J., Osborn, T.J., Briffa, K.R., Zorita, E., 2017. Internal and external forcing of Multidecadal Atlantic climate variability over the past 1,200 years. Nat. Geosci. 10 (7), 512–517. https://doi.org/10.1038/ngeo2962.
Weinkle, J., Landsea, C., Collins, D., Musulin, R., Crompton, R.P., Klotzbach, P.J., Pielke, R., 2018. Normalized hurricane damage in the continental United States 1900–2017. Nat. Sustain. 1 (12), 808–813. https://doi.org/10.1038/s41893-018-0165-2.
Winkler, T.S., van Hengstum, P.J., Donnelly, J.P., Wallace, E.J., Sullivan, R.M., MacDonald, D., Albury, N.A., 2020. Revising evidence of hurricane strikes on Abaco Island (the Bahamas) over the last 700 years. Sci. Rep. 10 (1) https://doi.org/10.1038/s41598-020-73132-x.
Winkler, T.S., van Hengstum, P.J., Donnelly, J.P., Wallace, E.J., D'Entremont, N., Hawkes, A.D., Maio, C.V., Sullivan, R.M., Woodruff, J.D., 2022. Oceanic passage of Hurricanes across cay Sal bank in the Bahamas over the last 530 years. Mar. Geol. 443, 106653 https://doi.org/10.1016/j.margeo.2021.106653.
Yang, W., Wallace, E., Vecchi, G.A., Donnelly, J.P., Emile-Geay, J., Hakim, G.J., Winkler, T.S., 2024. Last millennium hurricane activity linked to endogenous climate variability. Nat. Commun. 15 (1), 816.